Neuron 51, 811–822, September 21, 2006 ©2006 Elsevier Inc. DOI 10.1016/j.neuron.2006.09.006

Leptin Regulation of the Mesoaccumbens Dopamine Pathway

Stephanie Fulton,[1,3] Pavlos Pissios,[1] Ramon Pinol Manchon,[1] Linsey Stiles,[2] Lauren Frank,[2] Emmanuel N. Pothos,[2] Eleftheria Maratos-Flier,[1,*] and Jeffrey S. Flier[1,*]

[1] Department of Medicine and Division of Endocrinology
Beth Israel Deaconess Medical Center and
Harvard Medical School
Boston, Massachusetts 02115

[2] Department of Pharmacology and Experimental Therapeutics and
Program in Neuroscience
Tufts University School of Medicine
Boston, Massachusetts 02111

Summary

Leptin is an adipose-derived hormone that acts on hypothalamic leptin receptors to regulate energy balance. Leptin receptors are also expressed in extrahypothalamic sites including the ventral tegmental area (VTA), critical to brain reward circuitry. We report that leptin targets DA and GABA neurons of the VTA, inducing phosphorylation of signal-transducer-and-activator-of-transcription-3 (STAT3). Retrograde tracing combined with pSTAT3 immunohistochemistry show leptin-responsive VTA neurons projecting to nucleus accumbens (NAc). Assessing leptin function in the VTA, we showed that *ob/ob* mice had diminished locomotor response to amphetamine and lacked locomotor sensitization to repeated amphetamine injections, both defects reversed by leptin infusion. Electrically stimulated DA release from NAc shell terminals was markedly reduced in *ob/ob* slice preparations, and NAc DA levels and TH expression were lower. These data define a role for leptin in mesoaccumbens DA signaling and indicate that the mesoaccumbens DA pathway, critical to integrating motivated behavior, responds to this adipose-derived signal.

Introduction

The brain plays a critical role in the integration and regulation of physiologic systems controlling energy balance. Among the most important signals to the brain reporting the status of energy stores is the adipocyte-derived hormone leptin. Leptin potently regulates neural circuits controlling feeding, neuroendocrine function, metabolism, and body weight, and the absence of leptin (*ob/ob* mice) or its receptor (*db/db* mice) produces hyperphagia, endocrine/metabolic dysfunction, and profound obesity (Campfield et al., 1995; Halaas et al., 1995; Pelleymounter et al., 1995; Ahima et al., 1996). Leptin exerts its actions on energy balance through the long-form of the leptin receptor (ObRb), via signals including the JAK-STAT3 and PI-3 kinase pathways (Tartaglia et al., 1995; Baumann et al., 1996; Vaisse et al., 1996; Niswender et al., 2001; Zhao et al., 2002). The ability of leptin to activate STAT3 via ObRb has been most extensively studied in hypothalamus, and critical circuits involving leptin signals within POMC and NPY/AgRP neurons in the arcuate nucleus have been defined through functional neuroanatomy and genetic gain- and loss-of-function approaches (Erickson et al., 1996; Elias et al., 1999; Balthasar et al., 2004; Elmquist et al., 2005; Luquet et al., 2005).

ObRb mRNA expression in the CNS is not limited to the hypothalamus but includes expression within thalamus, cerebellum, and substantia nigra pars compacta among other areas (Elmquist et al., 1998). The presence of leptin receptor protein on midbrain dopamine (DA) neurons has also been reported (Hay-Schmidt et al., 2001; Figlewicz et al., 2003). DA neurons that originate in the VTA and project to the prefrontal cortex, amygdala, and ventral striatum are critical for the regulation of behavior, including feeding behavior. DA release in the nucleus accumbens (NAc), in particular, serves a fundamental role in learning about rewarding stimuli and behaviors and in the motor activity required to obtain rewards (Schultz, 2002; Kelley et al., 2005; Salamone et al., 2005). Moreover, the VTA-NAc dopamine pathway ("mesoaccumbens") has been extensively implicated in mechanisms of drug addiction, not only as the basis of the locomotor activating and reinforcing effects of certain drugs but also as a substrate for neuroadaptations that underlie the development and progression of addictive behaviors (Robinson and Berridge, 2003; Vezina, 2004; Hyman et al., 2006).

Leptin has been shown to modulate brain reward circuitry by altering performance for rewarding brain stimulation (Fulton et al., 2000, 2004). Leptin reverses the effect of food deprivation to reinstate drug-seeking behavior (Shalev et al., 2001), increases amphetamine-induced locomotion (Hao et al., 2004), and blocks conditioned place-preference for high-fat diet (Figlewicz et al., 2004). However, the role of leptin in midbrain DA function is poorly characterized, and actions of leptin on NAc DA signaling have not been demonstrated. We therefore sought to explore the potential impact of leptin action on the mesoaccumbens DA system through a combination of neuroanatomical, biochemical, behavioral, and electrochemical approaches in wild-type and leptin-deficient *ob/ob* mice. We found that leptin rapidly induces tyrosine phosphorylation of signal-transducer-and-activator-of-transcription-3 (STAT3), a key downstream mediator of leptin receptor signaling, in the VTA of *ob/ob* and wild-type mice. To characterize these leptin responsive VTA cells, we showed that pSTAT3 immunoreactive neurons colabeled with markers of DA and GABA. We then combined pSTAT3 immunohistochemistry with retrograde tract tracing and determined that a subset of leptin-responsive cells in the VTA

*Correspondence: emaratos@bidmc.harvard.edu (E.M-F.), jflier@bidmc.harvard.edu (J.S.F.)

[3] Present address: Department of Pharmacology, Center for Research in Neurological Sciences, Université de Montréal, Roger-Gaudry Building, Succursale Centre-ville, Montréal, Québec H3C 3J7, Canada.

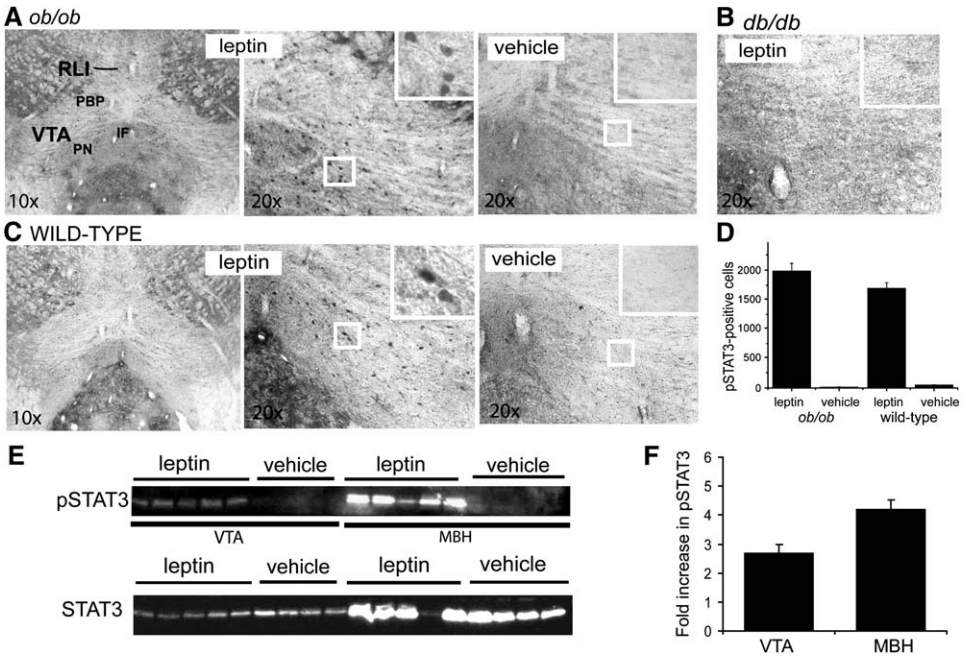

Figure 1. Peripheral Leptin Injection Increased pSTAT3 Expression in the VTA and Linear Raphe

(A) Immunohistochemical expression of pSTAT3 in *ob/ob* mice injected with leptin (5 mg/kg, i.p.) or vehicle (PBS; n = 4 per group).

(B) pSTAT3 expression was absent in leptin receptor-deficient *db/db* mice treated with leptin (n = 4).

(C) pSTAT3 immunoreactivity in wild-type mice administered leptin or vehicle (n = 4 mice per group).

(D) Estimates of pSTAT3-positive cells in the VTA and linear raphe (A10 region). There was no difference between *ob/ob* and lean wild-type mice ($F(1, 6) = 1.97$, $p > 0.05$). Estimates are based upon counts from one of two series.

(E) Western immunoblotting detection of pSTAT3 and total STAT3 in the VTA and MBH 90 min following acute leptin (5 mg/kg, i.p.) or vehicle injection in wild-type mice (n = 4–5 per group).

(F) Leptin induced a 2.63 ± 0.4-fold increase in pSTAT3 levels in the VTA and a 4.15 ± 0.8-fold increase in pSTAT3 in the mediobasal hypothalamus as compared to vehicle treated controls. Values are expressed as mean ± SEM.

project to the NAc. As the VTA-to-NAc pathway is critical for the locomotor-activating and sensitizing effects of drugs of abuse, we assessed the effects of leptin on d-amphetamine (AMPH)-induced locomotion and sensitization in both wild-type mice and *ob/ob* mice genetically deficient in leptin. *ob/ob* mice had diminished locomotor response to AMPH and showed no sensitization to repeated injection. Finally, to assess the impact of leptin deficiency on DA neurotransmission within the mesoaccumbens pathway, we analyzed electrically evoked DA release in the NAc, the expression of tyrosine hydroxylase (TH), the rate-limiting enzyme for DA biosynthesis, in the VTA and NAc, and levels of phosphorylated TH (ser40) and DA in the NAc of wild-type and *ob/ob* mice. A substantial impairment of DA release and biosynthetic capacity in the NAc was observed. Taken together, the findings define an important role for leptin action on the function of the mesoaccumbens DA pathway. The results have substantial implications for understanding the neural circuitry by which homeostatic and reward pathways may be integrated in the regulation of appetite, locomotor control, and body weight.

Results

Leptin Activates pSTAT3 in Dopaminergic Neurons in the VTA

We tested the ability of leptin to functionally activate leptin receptors in the VTA by examining the immunohistochemical expression of pSTAT3 in wild-type and ob/ob mice 2 hr after peripheral injection of leptin. Nuclear pSTAT3 labeling was found throughout the A10 dopamine region of the midbrain in both leptin-treated *ob/ob* and wild-type mice (Figures 1A and 1C). The most dense pSTAT3 labeling was visualized in the paranigral (PN) and interfascicular subnuclei (IF) of the VTA followed by more dorsal labeling in the rostral linear nucleus (RLi) of the raphe. To a lesser extent, nuclear staining was also observed in the parabrachial pigmented nucleus (PBN) of the VTA and the caudal linear nucleus (CLi) of the raphe. Nuclear pSTAT3 labeling in the VTA, RLi, and CLi was counted in half of all brain slices collected (1-in-2 series).There was no significant difference between estimates of pSTAT3-positive cells in the A10 region between wild-type and *ob/ob* mice following leptin administration (Figure 1D). Labeling was absent in leptin-receptor-deficient *db/db* mice after leptin administration, which demonstrates the obligatory role of ObRb (Figure 1B). To quantitate pSTAT3 protein, we carried out western immunoblotting on VTA microdissections (Figure 1E). As a major target of leptin action is the mediobasal hypothalamus (MBH) which includes the arcuate, ventromedial, and dorsomedial nuclei, we also measured induction of pSTAT3 in MBH tissue samples for comparative analyses. As shown in Figure 1F, the magnitude of leptin-induced pSTAT3 in the VTA at 90 min after leptin injection was an average of 63% of that

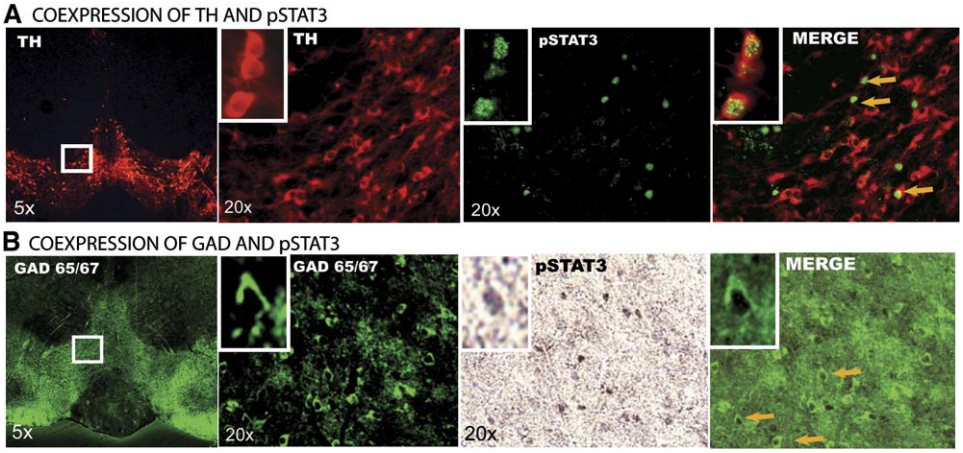

Figure 2. Leptin-Induced pSTAT3 Immunoreactivity Colocalizes with Dopamine and GABA

(A) Representative photomicrographs of the VTA showing TH and pSTAT3 immunofluorescence in an *ob/ob* mouse. There was no difference in the estimates of TH-labeled cells between *ob/ob* (800.3 ± 51.7) and wild-type mice (836 ± 93.3) as measured from a subset of coronal slices ($F(1, 6) = .263$, $p > 0.05$) (n = 4 mice/group). Note by the merged images that pSTAT3 nuclear immunoreactivity (green) colocalizes with cytoplasmic TH expression (red). TH-labeled neurons represent 42% ± 4.7% of pSTAT3-positive cells.

(B) Photomicropgraphs of the VTA illustrating GAD cytoplasmic immunofluorescence (green) and pSTAT3 nuclear staining (DAB). Note that there is colocalization of pSTAT3 and GAD IHC. Cells labeled with GAD accounted for 23% ± 5.1% of pSTAT3 staining in this region. Values are expressed as mean ± SEM.

observed in the MBH and a lesser signal was seen at 60 min after injection (data not shown).

The VTA is populated by both DA and GABA neurons. We therefore sought to determine whether either of these cell types respond to leptin by colabeling pSTAT3 with antibodies to tyrosine hydroxylase (TH) and glutamate decarboxylase (GAD). Estimates of the number of TH-labeled neurons did not reveal any significant differences between saline-injected *ob/ob* and wild-type mice, thus complete leptin-deficiency does not seem to be associated with an altered number of DA neurons in the A10 region. As shown in Figure 2A, pSTAT3 nuclear labeling was present in neurons expressing TH. Neurons coexpressing TH and pSTAT3 account for 42% ± 4% of pSTAT3-positive cells. Double-labeled neurons were found predominantly in the PN subpopulation of the VTA and to a lesser extent the RLi and CLi. Neighboring GABA neurons of the VTA are known to have an inhibitory influence on DA neurotransmission, and thus we colabeled for the enzyme GAD which is required for GABA synthesis. Neurons coexpressing GAD and pSTAT3 represented 23% ± 5% of total pSTAT3-positive cells and were seen primarily in the VTA.

VTA Neurons Expressing pSTAT3 Project to the Nucleus Accumbens

The largest projection of A10 dopamine neurons is to the NAc (Beckstead et al., 1979; Swanson, 1982), and this pathway is important for modulation of goal-oriented behavior and the effect of systemically administered drugs. There is evidence that separate populations of VTA dopamine neurons innervate the NAc and the prefrontal cortex (Sesack and Carr, 2002). To determine whether pSTAT3-positive VTA cells send projections to the NAc, we combined in vivo retrograde tracing from the NAc with immunohistochemistry. Of the 14 mice injected with the tracer, the injection sites of eight mice were confirmed to be in the NAc core and/or shell (Figure 3A). Microbead tracers do not diffuse significantly from the site of injection, and histological analysis showed that the fluorescent beads were contained around the tip of the micropipette in the eight mice. In these eight mice, the tip of the micropipette was positioned in the NAc at the level of 1.18 to 1.40 (mm anterior Bregma). In all eight mice, pSTAT3 immunoreactivity was present in retrogradely labeled perikarya of the VTA. The mean percentage of rhodamine labeled cells that expressed pSTAT3 was 12% ± 2%.

Leptin Enhances Sensitization to Amphetamine

Amphetamine (AMPH) increases extracellular DA in the terminal and cell-body regions of midbrain DA neurons either through inhibition of DA reuptake or reverse transport of cytosolic DA through the DAT transporter. Elevated extracellular DA in the NAc is associated with AMPH-induced locomotor activity (Kalivas and Stewart, 1991; Heusner et al., 2003). Furthermore, the process whereby animals become more sensitive to the locomotor-activating effects of amphetamine upon repeated injections ("sensitization") is secondary to neuroadaptations of midbrain DA neurons (Vezina, 2004). Thus, to determine whether leptin has effects on behavioral outcomes directly involving the mesoaccumbens DA pathway, we examined the influence of peripheral leptin infusion on AMPH-induced locomotion. Figure 4A outlines the experimental procedure. Mice were initially acclimatized in dummy activity-monitoring chambers and then were implanted with 14 day osmotic minipumps that infused leptin (500 ng/hour; 12 μg/day) or PBS subcutaneously. This dose of leptin reverses the metabolic phenotype of *ob/ob* mice (Halaas et al., 1997) and slightly exceeds the lowest dose of leptin (10 μg/day) that decreases food intake and body weights in wild-type C57BL/6J mice (Harris et al., 1998). Mean body weights immediately after pump implantation were 24 ± 1.4 g (*ob/ob*—leptin), 24.8 ± 1 g (*ob/ob*—vehicle),

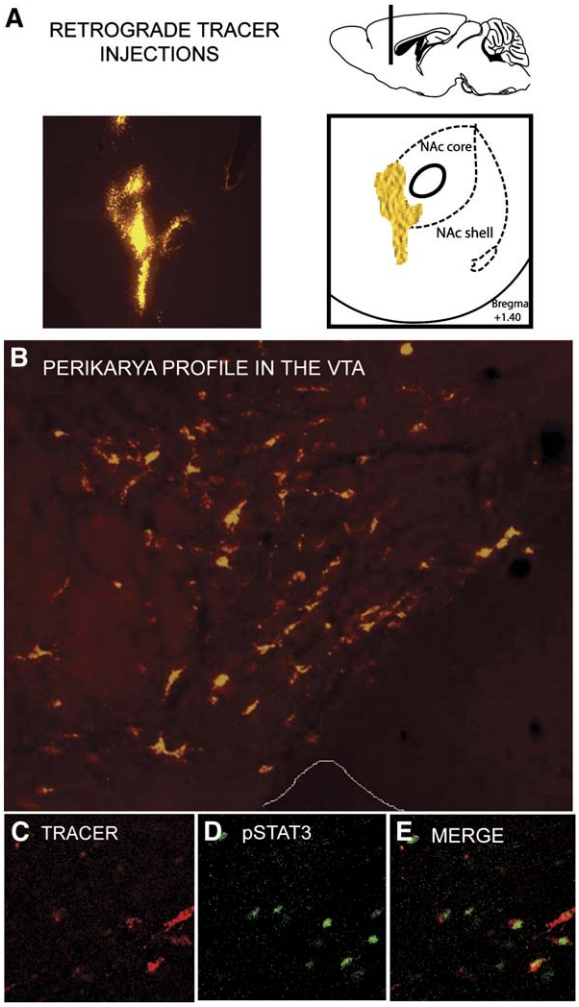

Figure 3. Leptin-Induced pSTAT3 Immunoreactivity in the VTA Colocalizes with a Tract Tracer Retrogradely Transported from the Nac

(A) Illustration and photomicrograph showing a representative injection site of the rhodamine microbeads. Injection sites for 8 of the 14 mice were in the NAc.

(B) Photomicrograph depicting the profile of retrogradely labeled cells in the VTA.

(C) Confocal image of tracer labeling in the VTA.

(D) Confocal image of nuclear pSTAT3 immunofluorescence.

(E) Confocal image depicting colocalization of pSTAT3 (green) and rhodamine microbead tracer (red). pSTAT3-positive cells accounted for an average of 12% ± 2% of rhodamine-labeled cells.

18.9 ± 0.4 g (wild-type—leptin), and 19.6 ± 0.4 g (wild-type—vehicle). Following 10 days of continuous leptin infusion, average body weights were 26.8 ± 0.8 g (*ob*/*ob*—leptin), 32.6 ± 0.9 g (*ob*/*ob*—vehicle), 20.6 ± 0.6 (wild-type—leptin), and 23.2 ± 0.7 g (wild-type—vehicle). Locomotor activity was measured for 4 hr following IP injections of (1) saline, (2) 1 mg/kg AMPH, (3) 4 mg/kg AMPH and, (4) 1 mg/kg AMPH dose, each separated by 3 days. Locomotor activity counts collected during the first hour after injection were used for all comparisons.

Following injection, locomotor activity was assessed during the light phase of the circadian cycle since all our biochemical assays were carried out in mice during the light cycle phase. After initial saline injection, activity was low in all groups (Figure 4B). Three days later, low-dose (1 mg/kg) AMPH injection elicited no increase in locomotor activity compared to saline treatment for any group, confirming that this is a subthreshold dose. Three days after low-dose AMPH, high-dose AMPH resulted in a robust induction of locomotor activity, the degree of which was genotype and treatment specific (Figures 4D and 4F). First, the locomotor response to high-dose AMPH (4 mg/kg) was lower in *ob*/*ob* mice: activity of vehicle-infused *ob*/*ob* mice was on average 36% lower as compared to vehicle-infused wild-type mice. Further, leptin infusion markedly enhanced the locomotor response to high-dose amphetamine in both groups, with the incremental response after leptin infusion being greater in *ob*/*ob* mice compared to control mice. Following high-dose AMPH, animals were again treated with low-dose AMPH to examine sensitization. The degree of AMPH sensitization was determined by comparing activity counts from the first hour after the initial low-dose AMPH to those collected after the second low dose of AMPH. Wild-type mice showed a 3- to 4-fold increased response to the second low dose of AMPH, confirming AMPH sensitization, both in the presence and absence of leptin infusion (Figures 4E and 4G). In *ob*/*ob* mice infused with vehicle, there were no significant differences between the two low-dose AMPH conditions, confirming absence of sensitization to AMPH and suggesting dysregulation of the mesoaccumbens pathway in these mice. Remarkably, leptin infusion fully restored the behavioral sensitization to AMPH in *ob*/*ob* mice, producing a 3.1-fold increase in activity in response to the second dose of AMPH relative to the first low dose (Figure 4G).

Leptin Replacement Elevates TH Levels in the VTA and NAc of *ob*/*ob* Mice

To evaluate potential mechanisms underlying the observed difference in amphetamine-induced locomotion and behavioral sensitization between leptin-deficient *ob*/*ob* and wild-type mice, we next investigated molecular pathways underlying DA synthesis. TH is the rate-limiting enzyme in DA synthesis. We measured protein levels of TH in the VTA and NAc after 3 day minipump infusion of leptin (500 ng/hr) or vehicle (PBS) via western immunoblotting. In *ob*/*ob* mice, 3 day leptin infusion increased TH protein concentrations in the VTA by 2.5-fold as compared to vehicle-treated controls (Figures 5A and 5C). In contrast, leptin administration failed to alter TH levels in the MBH, another region where TH is expressed (Figure 5B). In the NAc terminal region, TH was reduced in *ob*/*ob* controls as compared to wild-type controls, whereas leptin replacement reversed this effect by increasing TH levels 2.2-fold relative to saline-treated *ob*/*ob* mice (Figure 5C). Changes in the state of phosphorylation of TH are critically involved in the regulation of DA synthesis. In particular, increases in phosphorylation of Ser40 is associated with increased enzymatic activity of TH (Harada et al., 1996; Jedynak et al., 2002). As shown in Figure 5D, leptin treatment of *ob*/*ob* mice increased phosphoTH (ser40) levels by an average of 28.2% and 46.2% in the NAc as compared to leptin- and vehicle-treated wild-type mice, respectively.

As there was no difference in the number of TH immunoreactive neurons between *ob*/*ob* and wild-type mice

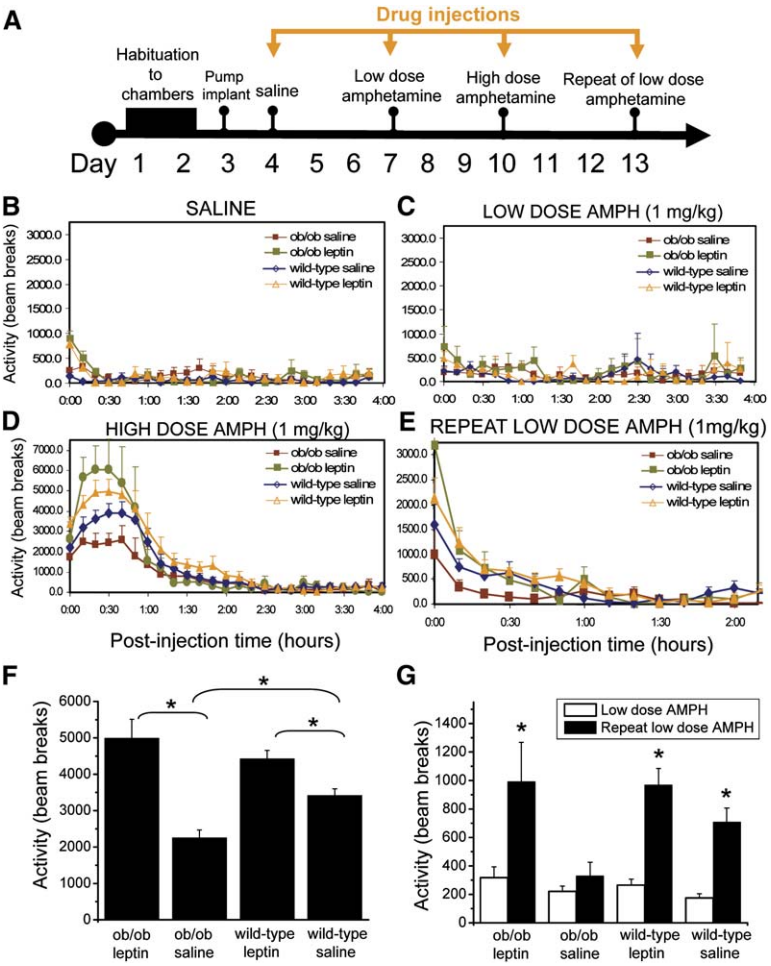

Figure 4. Chronic Leptin Infusion Enhances Amphetamine-Induced Locomotor Activity and Sensitization

(A) Amphetamine sensitization procedure for *ob*/*ob* and wild-type mice receiving continuous infusion of leptin (500 ng/hr, SC) or PBS for 13 days (n = 5–8 per group).

(B) Locomotor activity following saline injection.

(C) A subthreshold dose of amphetamine did not increase locomotor activity.

(D and F) The high dose of amphetamine augmented locomotor activity in all groups. Locomotor activity of vehicle-infused *ob*/*ob* mice was reduced as compared to vehicle-treated wild-type mice ($F(1, 82) = 18.38$, $p = 0.001$). Leptin treatment more than doubled activity levels in *ob*/*ob* ($F(1, 58) = 18.38$, $p < 0.0001$) and produced a 30% increase in wild-type mice ($F(1, 94) = 18.38$, $p = 0.003$) as compared to respective vehicle controls.

(E and G) The locomotor-sensitizing effects of repeated AMPH injection were absent in vehicle-infused *ob*/*ob* mice. Relative to the first low dose of AMPH, activity levels were not elevated after the second low dose of AMPH in vehicle-infused *ob*/*ob* mice ($F(1, 58) = 0.78$, $p = 0.38$) whereas there was a 4-fold increase in vehicle-infused wild-type mice ($F(1, 64) = 16.51$, $p < 0.0001$), a 3.7-fold increase in leptin-infused wild-type mice ($F(1, 70) = 18.04$, $p < 0.0001$) and a 3.1-fold increase in leptin-treated *ob*/*ob* mice ($F(1, 39) = 4.03$, $p = 0.05$). Values are expressed as mean ± SEM. All statistics were computed by ANOVA with Fisher's post-hoc comparison. *$p < 0.05$.

(Figure 2), this suggests that the differences in VTA and NAc TH and DA levels reflect changes in protein levels per neuron.

Mice Lacking Leptin Have Diminished Evoked Dopamine Release

To further evaluate DA dysregulation, we directly assessed DA release using electrochemical methods to measure evoked DA release in acute coronal slices of *ob*/*ob* and wild-type mice. A carbon fiber electrode inserted into the NAc shell was used to collect amperometric recordings from dopaminergic axons arising from the VTA. An adjacent bipolar electrode delivered single pulses (0.5 mA, 2 ms) to trigger the release of synaptic DA. The current caused by the electrochemical oxidation of the extracellular DA serves as a measure of DA release kinetics in real time. As shown in Figures 6A and 6B, the evoked DA signal in *ob*/*ob* mice was reduced by on average 90% as compared to the signal measured in wild-type mice. Real-time DA kinetics are primarily determined primarily by exocytosis and rate of reuptake, so to determine which of these factors contribute to reduced DA signal in *ob*/*ob* mice, we examined both the width of the recorded current spike and the effect of the DA reuptake blocker nomifensin, a DA transporter (DAT)-specific inhibitor, on current amplitude and width. The spike width of the recorded current was similar between *ob*/*ob* and wild-type controls in the absence of nomifensine. In addition, 30 min bath application of nomifensine did not eliminate the reduction of DA signal amplitude in ob mice. These data suggest that the rate of DA reuptake is similar between the two genotypes and that reduced DA signal in *ob*/*ob* mice is due to diminished synaptic DA release. As an additional assessment, we measured DA release following a pattern of stimulation pulses that approximates real-time firing conditions (Figure 6E). As shown in Figure 6F, there was a progressive decrease in the mean amplitude of DA release in wild-type mice. In contrast, there was a much lower mean amplitude of DA release in *ob*/*ob* mice that remained relatively constant over the five stimulation pulses (Figure 6G).

To assess whether presynaptic DA levels were indeed lower in the NAc of *ob*/*ob* mice relative to wild-type mice, we measured DA levels via radioimmunoassay of NAc tissue dissections. As illustrated in Figure 6E, NAc DA levels were on average 47% lower in *ob*/*ob* mice as compared to wild-type mice. These data are consistent with our observations of reduced TH expression in *ob*/*ob* mice.

Discussion

The adipocyte hormone leptin acts directly on CNS circuits to influence appetite, energy expenditure, neuroendocrine function, and other processes. The best

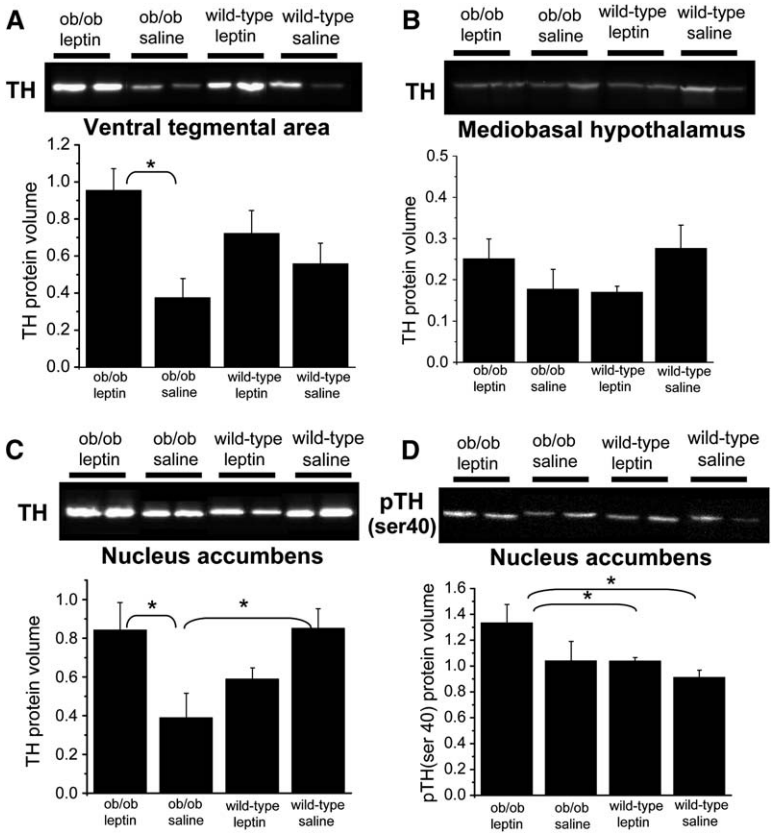

Figure 5. Leptin Infusion Increases TH Levels in the VTA and NAc and Increases the Expression of Phosphorylated TH ser40 in the NAc of *ob/ob* Mice

(A) Three day leptin infusion (500 ng/hr) in *ob/ob* mice increased TH levels in the VTA by 2.5-fold relative to vehicle-treated *ob/ob* mice (n = 8–12 per group) ($F(3, 40) = 3.98$, $p = 0.014$).

(B) Leptin infusion failed to alter TH levels in MBH samples ($F(3, 18) = 1.50$, $p = 0.24$).

(C) TH protein levels in the NAc of *ob/ob* mice were elevated 2.2-fold by leptin relative to controls ($F(1, 14) = 3.98$, $p = 0.007$). Vehicle-infused *ob/ob* mice had 54% less NAc TH than wild-type controls (n = 7–8 per group) ($F(3, 27) = 3.98$, $p = 0.008$).

(D) Leptin increased phosphoTH (ser40) levels in the NAc of *ob/ob* mice by 28.2% relative to leptin-treated wild-type mice and by 46.2% as compared to saline-treated wild-type mice (n= 6–8 per group) ($F(3, 25) = 3.36$, $p = 0.035$). Values for immunoblotting are arbitrary units. All values are expressed as mean ± SEM. Statistics were computed by ANOVA with Fisher's post hoc comparisons. *$p < 0.05$.

characterized direct targets of leptin action in the CNS are within the hypothalamus, most specifically the arcuate nucleus and ventromedial hypothalamus. Although the signaling form of the leptin receptor, ObRb, is expressed more widely in the CNS, potential actions of leptin on extrahypothalamic circuits have not as yet been clearly linked to function. The mesoaccumbens DA pathway plays a role in incentive motivation (Berridge and Robinson, 1998; Kelley et al., 2005; Robinson et al., 2005; Salamone et al., 2005) and reward-related learning (Tobler et al., 2005), and is a major substrate underlying the locomotor-activating, rewarding and addictive effects of drugs of abuse (Wise, 2002; Kelley, 2004; Vezina, 2004). In the present study, we demonstrate that leptin directly targets TH and GABA neurons within the mesoaccumbens pathway and has actions consistent with an ability to modulate DA tone in this circuit. In aggregate, these observations reveal a mechanism by which leptin may directly influence brain reward circuitry and suggests that modulation of midbrain DA as a consequence of leptin action is one way in which leptin may influence behaviors relevant to energy homeostasis.

After peripheral injection of leptin, tyrosine phosphorylation of STAT3 was identified in the VTA both by western blotting and by immunohistochemical analysis, with the latter demonstrating colocalization of pSTAT3 in a subset of DA neurons of the VTA . In all previous studies, leptin-induced pSTAT3 in neurons is taken to indicate a direct action of leptin, mediated by the long form of the leptin receptor (ObRb) on the responsive cell. In fact, ObRb protein has been colocalized with TH in VTA neurons (Figlewicz et al., 2003), and ObRb coexpression in VTA DA neurons has been demonstrated using a genetic strategy in which ObRb IRES-Cre mice are crossed to Rosa26-EYFP reporter mice to generate ObRb-EYFP reporter mice (J. Lachey, J. Friedman, and J. Elmquist, personal communication). Localization of pSTAT3 to DA neurons was most prominent in mid A10 regions including the paranigral nucleus and linear raphe. Dopaminergic neurons of the paranigral subregion of the VTA are known to richly innervate the NAc (Phillipson and Griffiths, 1985). Indeed, we found that a retrograde tracer injected into the Nac-labeled VTA perikarya that expressed pSTAT3 demonstrating that at least a subset of the VTA leptin-regulated neurons innervate the NAc. We also identified a smaller subset of pSTAT3-immunoreactive cells that were colabeled with a marker for GABA, the second major neurotransmitter found in the VTA. As several lines of evidence suggest that VTA GABAergic neurons have an inhibitory influence on DA neurotransmission, regulation of GABA is an additional mechanism by which leptin might alter DA function.

To link the ability of leptin to activate STAT3 in VTA DA neurons to a behavioral phenomenon contingent on mesoaccumbens DA neurotransmission, we examined the ability of leptin deficiency and treatment to alter amphetamine-induced locomotion. One of the principle actions of amphetamine is to increase extracellular levels of DA through blocking reuptake and reversing DA transport via the dopamine transporter. These actions of amphetamine in the NAc are associated with its ability to enhance locomotor activity (Hoebel et al., 1983; Heusner et al., 2003), whereas its actions in the VTA are associated with the induction of behavioral sensitization

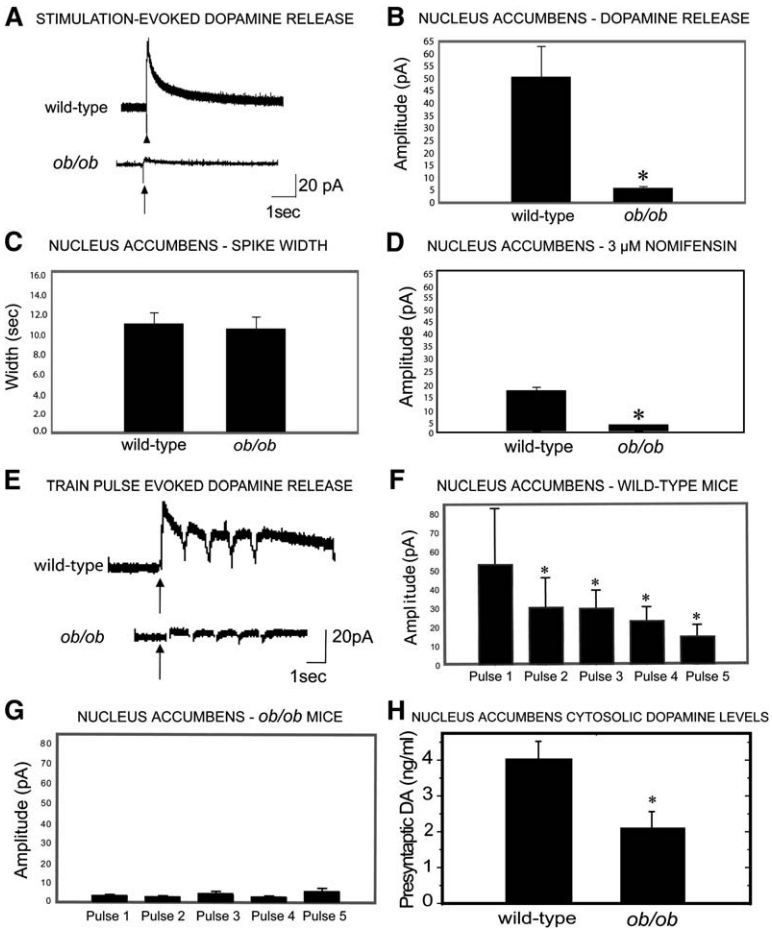

Figure 6. Reduced Evoked DA Release in the NAc of *ob/ob* Mice

(A) Representative amperometric traces of electrical stimulation-evoked dopamine release in acute coronal accumbens slices from *ob/ob* and wild-type mice. Stimulation electrodes and carbon fiber recording microelectrodes were positioned in the shell region of the posterior nucleus accumbens, which receives the majority of the dopaminergic projections from the VTA. Data were acquired at 50 kHz and digitally postfiltered at 1 kHz. Arrows point to onset of electrical single pulse (2 ms of 0.5 mA).

(B) The mean evoked dopamine signal amplitude was significantly reduced from 50 ± 12 pA (mean ± SEM) in wild-type slices to 5 ± 1 pA in *ob/ob* slices (n = 25 stimulations in seven slices/mice per genotype, (F(1, 46) = 11.97, *p < 0.01 by one-way ANOVA).

(C) Mean signal width was not different, suggesting that dopamine reuptake rate did not change in *ob/ob* slices.

(D) In the presence of the DAT-specific reuptake blocker nomifensin, the reduction in evoked dopamine signal was maintained, further indicating that the signal reduction is due to a difference in evoked release and not to an increase in DA reuptake. *p < 0.01.

(E) Representative amperometric traces from 300 μm nucleus accumbens slices following a train of five electrical pulses of 500 μA each with an interpulse interval of 500 ms. These traces were used to determine the mean amplitude for each pulse in *ob/ob* mice and wild-type controls.

(F and G) There was a significant and progressive decrease in the mean amplitude for wild-type mice (F(33, 4) = 130.1541, *p < 0.01) while the *ob/ob* mice had an overall lower mean amplitude, which, however, remained stable throughout the five train pulses.

(H) As measured by radioimmunoassay of NAc microdissections, cytosolic DA levels were on average 47% lower in *ob/ob* mice relative to wild-type mice (F(1, 22) = 7.8, p = 0.01). All values are expressed as mean ± SEM.

(Vezina, 2004). Basal locomotor activity did not differ between any of the genotypes or treatment groups after saline or the first low-dose amphetamine injection. This reflects the low basal locomotor activity during the light phase of the circadian cycle and indicates that the different responses between genotypes and treatment groups (see below) were not due to differences in basal activity. The locomotor response to high-dose amphetamine was substantially diminished in *ob/ob* mice relative to the wild-type mice. Peripheral leptin infusion at doses in the physiological range reversed this defect and elevated amphetamine-induced locomotor activity in *ob/ob* to levels above that observed in any of the other treatment groups. Leptin infusion increased locomotion in wild-type mice as well, although to a smaller extent.

Remarkably, in addition to an attenuated locomotor response to high-dose amphetamine, *ob/ob* mice showed no behavioral sensitization to repeat low-dose amphetamine injection. Unlike wild-type mice, which displayed the expected enhanced locomotor response to a second low dose of amphetamine, saline-treated *ob/ob* mice had no increased locomotor activity following a repeat low-dose amphetamine injection as compared to that after the first low-dose injection. Strikingly, leptin treatment of *ob/ob* mice completely reversed this deficiency, as leptin treated *ob/ob* mice had a sensitized locomotor response similar to that in wild-type mice. These data highlight a critical role for leptin in the development of AMPH sensitization and thus the reorganization of neural circuits that underlies the sensitization process. Linked to the sensitizing effects of drugs of abuse such as cocaine and AMPH are alterations in gene transcription and increased dendritic branching of medium spiny neurons of the NAc (Robinson and Berridge, 2003; Hyman et al., 2006).The requirement of leptin for AMPH sensitization suggests a role for leptin in such molecular and morphological adaptations.

To explain the diminished amphetamine-induced locomotor response of *ob/ob* mice, we sought to determine whether leptin deficiency is associated with altered DA release in the mesoaccumbens pathway. There is prior evidence in rats that AMPH-induced changes in NAc DA release correlate with the presynaptic DA levels (Pothos et al., 1998). TH protein levels, both in VTA cell body and NAc terminal regions, were reduced in *ob/ob* mice as compared to leptin-infused *ob/ob* mice. In addition, leptin replacement in ob/ob mice increased levels of TH and phosphorylated TH ser40 in the NAc.

To directly probe DA release in the NAc, we measured the amount of evoked-DA release from NAc terminals in acute slice preparations of *ob/ob* and wild-type mice.

Amperometric recordings detected dramatically lower DA signal in *ob*/*ob* mice relative to wild-type mice in response to both a single electrical pulse or a train of pulses. Moreover, during the train of electrical pulses that resembles real-time firing of DA neurons, the amplitude of DA release did not progressively decrease in *ob*/*ob* mice as it did in wild-type mice. Under normal conditions DA release is rapidly reduced via the actions of the D2 autoreceptor (Farnebo and Hamberger, 1971). That the amplitude of DA release remained relatively constant over stimulation pulses in *ob*/*ob* mice suggests that mechanisms underlying D2 autoreceptor function may be disabled in *ob*/*ob* mice. Despite impairments in DA release in *ob*/*ob* mice, the rate of DA clearance did not differ between genotypes, suggesting that mechanisms controlling DA reuptake are not responsible for the observed defects in DA release in *ob*/*ob* mice. Therefore, diminished evoked DA release in *ob*/*ob* mice is at least partially due to a reduction in DA available for release, potentially due to diminished synthesis. Consistent with this possibility, DA levels measured in NAc punches were reduced by 47%. It remains to be elucidated however whether additional mechanisms influencing DA release in the NAc could also be impaired in *ob*/*ob* mice.

It is well known that *ob*/*ob* mice lacking leptin have reduced locomotor activity, and this can be corrected with leptin therapy (Pelleymounter et al., 1995), but the neural circuitry underlying this effect is not well described. Might this be related to our finding that *ob*/*ob* mice have reduced locomotor response to amphetamine which is reversed by leptin therapy? Amphetamine is well known to induce hyperlocomotion in mice, and this is associated with the action of amphetamine on DA within the NAc. Recent studies using genetic approaches to prevent DA synthesis and restore this within specific brain regions strongly support the notion that the locomotor effect of amphetamine requires DA synthesis, and DA synthesis in the NAc is sufficient to confer this response (Heusner et al., 2003). Thus, our finding that *ob*/*ob* mice have reduced locomotor responses to amphetamine and reduced DA release in the NAc are fully consistent with these conclusions. It remains to be determined to what extent this neural circuit is responsible for the overall suppression of locomotor activity consequent to leptin deficiency in *ob*/*ob* mice.

The role of neurotransmitter systems within the NAc in reward and addiction has been the subject of much investigation (Di Chiara et al., 2004; Kelley et al., 2005; Salamone et al., 2005). Functional inhibition of the NAc shell via GABA agonism produces intense hyperphagia in ad libitum fed animals (Kelley et al., 2005), while dietary obese rats have low basal extracellular DA levels in the NAc (Pothos et al., 1998). These observations are consistent with our findings that hyperphagic *ob*/*ob* mice have reduced DA signaling in the NAc. How does this finding relate to existing concepts of the role of DA in the regulation of feeding? Much of the literature on the subject originates in studies with drugs of abuse, not feeding and natural reinforcers. Those studies that have focused on the link between mesoaccumbens dopamine and normal feeding report that mesoaccumbens extracellular dopamine increases during the appetitive and/or consummatory phase of feeding, and in some cases it outlasts the consummatory response (Hernandez and Hoebel, 1988; Pothos et al., 1995; Martel and Fantino, 1996; Bassareo and Di Chiara, 1999; Ahn and Phillips, 2002; Hajnal et al., 2004). One interpretation of such findings is that mesoaccumbens dopamine release is a signal associated with food-related learning especially as it pertains to satiation. Evidence directly linking reduced mesoaccumbens DA signaling with obesity is limited. Basal extracellular dopamine in the NAc is low in rats with dietary obesity, and this is consistent with the hypothesis that these animals compensate for a deficit in NAc DA by increasing food intake (Pothos et al., 1998). The hypothesis that decreased NAc dopamine signaling leads to increased feeding is compatible with the finding that obese humans have reduced central D2 receptor levels (Wang et al., 2001) and that administration of DA agonists to *ob*/*ob* mice normalizes hyperphagia (Scislowski et al., 1999; Bina and Cincotta, 2000). Therefore, it is possible to hypothesize that mesoaccumbens dopamine release and signaling in the leptin deficient *ob*/*ob* mouse are too low to serve as an adequate reward-relevant learning and satiety signal. Based on the studies presented here, a defect in NAc dopamine release may now be attributed at least partly to deficient leptin action upon this circuit. Since chronic leptin administration reduces food intake, increases energy expenditure, and promotes weight loss, and these in turn can affect other metabolic and neural signals, it is possible that the actions of leptin on the mesoaccumbens pathway responsible for the enhancement of amphetamine-induced locomotion are both direct, via actions on the VTA-NAc circuit described here, and indirect. The extent to which this results from direct leptin action on neurons within the mesoaccumbens circuit, as opposed to indirect effects via changes in other hormones or neuropeptides, will require additional study.

In summary, we have defined a direct action of peripheral leptin to induce signaling in neurons within the mesoaccumbens DA circuit. In leptin-deficient *ob*/*ob* mice, deficient leptin action causes reduced NAc TH levels and reduced evoked DA release from coronal slices of NAc shell. Finally, these neuroanatomic and biochemical findings are accompanied by important behavioral consequences previously linked to this circuit, since leptin action regulates the ability of AMPH to stimulate locomotor activity and leptin is required for sensitization of the locomotor response to low-dose amphetamine. Taken together, these data suggest that the actions of leptin go beyond well-known targets in the hypothalamus and brainstem and that the modulation of mesoaccumbens DA circuitry by leptin may be important for the regulation of behaviors that influence appetite, locomotor control, and body weight.

Experimental Procedures

Subjects

Male B6.V-*Lep*^{ob}/J (*ob*/*ob*), wild-type controls (*Lep*$^{Ob+/?}$), *Lepr*^{db} (*db*/*db*), and wild-type mice all on a C57BL/6J background were purchased from Jackson Laboratory. Mice, between 4 and 10 weeks of age, were housed in a temperature- and humidity-controlled room that was maintained on a 14:10 light/dark cycle, with lights on at 0600 hr. All experiments were conducted in accordance with the guidelines and approval of the Harvard Medical School and Beth

Israel Deaconess Medical Center and Tufts University-New England Medical Center Institutional Animal Care and Use Committees.

Immunohistochemical Characterization of Leptin Signaling

Recombinant mouse leptin was obtained from Dr. A.F. Parlow (National Hormone and Peptide Program, National Institute of Diabetes and Digestive Kidney Diseases, Torrance, California). Leptin (5 mg/kg body weight) or vehicle (PBS) was injected i.p. following an overnight fast. Two hours after injection, mice were anesthetized with ketamine/xylazine (45 mg/kg/5 mg/kg, i.p.) and perfused transcardially with ice-cold saline followed by 10% neutral buffered formalin. Brains were removed and postfixed for 4–8 hr and then cryoprotected by overnight immersion in a 20% sucrose solution. Frozen brains were sliced in 25 μm coronal sections using a microtome. For pSTAT3 immunohistochemistry, free-floating sections were pretreated with 1% NaOH, 1% H_2O_2, and then 0.6% glycine, blocked in goat serum, and then incubated in anti-pSTAT3 (tyr705) antibody (1:1000, Cell Signal Technology) for 48–54 hr at 4°C. Sections were rinsed and incubated with a secondary biotinylated anti-rabbit antibody (1:1000; Vector Laboratories), labeled with avidin-biotin complex, and then stained with nickel-enhanced diaminobenzidine. For double-labeling experiments examining the cell types expressing pSTAT3 in the VTA, separate series of brain sections were additionally processed with a mouse monoclonal antibody to TH (1:1000; Chemicon International) or a rabbit polyclonal antibody to $GAD^{65/67}$ (1:1000; Chemicon). Fluorescent secondary detection Alexafluor 595 and 488 (1:200, Vector Laboratories) was used to visualize TH and $GAD^{65/67}$, respectively. Brain sections for light microscopy were mounted on gelatin-coated slides, dehydrated, and coverslipped with mounting solution. Fluorescently labeled sections were mounted and coverslipped with aqueous mounting medium for fluorescence. Staining was visualized using a Zeiss Axio Imager A1 fluorescent microscope with an Axiocam HR cooled CCD digital camera and Axiovision 4AC image acquisition software (Carl Zeiss Microimaging, Inc.). Estimates of pSTAT3-labeled cell numbers were made by counting nickel-enhanced DAB nuclear staining in the midbrain area corresponding to the A10 dopamine cell group based upon the description by Dahlstrom and Fuxe (1964) and its application to C57BL/6J mice (Zaborszky and Vadasz, 2001). Accordingly, the A10 cell group includes the VTA, RLi, and CLi. Nuclear pSTAT3 was manually counted in the VTA, RLi, and CLi in every mounted section of a 1-in-2 series using Image J software (Rasband, WS; Image J, US, NIH). For TH and pST T3 double labeling, the number of TH-positive neurons was counted in coronal sections that correspond to five rostrocaudal levels of the A10 DA region as based on the mouse atlas of Paxinos and Franklin (2001) (distance caudal to Bregma): −3.08 mm, −3.16 mm, −3.40 mm, −3.64 mm, 3.80 mm. Percentages of pSTAT3-positive cells that colocalized with TH or GAD immunoreactivity were derived from sections corresponding to these same five coronal levels.

Subcutaneous Leptin Infusion

Leptin infusion for either 3 days (western blotting) or 14 days (behavioral testing) was delivered using Alzet micro-osmotic pumps (Alta Corp.). Pumps were filled with either leptin (500 ng/hr; 12 μg/day) or vehicle (PBS) and primed for 4–6 hr at 37°C before implantation. The pump was inserted into the interscapular region under Isoflurane anesthesia. The incision was closed with wound clips.

SDS-PAGE and Immunoblotting

Animals were anesthetized with CO_2 before decapitation. Brains were rapidly removed and froze on powdered dry ice. Frozen brains were placed in a cold aluminum brain slicer with 0.5 mm dividers. A 1 mm thick frozen coronal section limiting the VTA and 2 mm coronal section containing the arcuate, ventromedial, and dorsomedial nuclei ("mediobasal hypothalamus") was sliced and mounted on a slide. Brain nuclei were rapidly microdissected using a brain punch set (Stoelting Co). Two tissue punches, one for each hemisphere, were collected for the VTA (0.75 mm diameter), and the MBH (1.0 mm diameter). Microdissected tissues were homogenized on ice in 100 μl of cell lysis buffer (20 mM Tris [pH 7.5], 150 mM NaCl, 1 mM Na_2EDTA, 1 mM EGTA, 1% Triton, 2.5 mM sodium pyrophosphate, 1mM β-glycerophosphate, 1mM Na_3VO_4, 1 μg/ml leupeptin) with added protease (PMSF 100 μM) and phosphatase inhibitors (Sigma phosphatase inhibitor cocktails I and II) in 1.5 ml tubes using a motorized pestle. Tubes containing the homogenates were shaken for 30 min at 4°C to allow for complete lysis and then centrifuged for 15 min at 14,000 × g. Protein concentrations were measured using BCA protein assay (Pierce Biotechnology). For the experiment examining pSTAT3 protein levels following IP leptin (5mg/kg body weight) or vehicle (PBS), 70 μg of protein was loaded into 10% polyacrylamide gels. Protein of concentration representing 50%, 100%, 150% of sample protein concentrations from saline-treated wild-type mice served as standards for each gel. Protein was transferred overnight (30V) onto PVDF membranes using transfer buffer (50 mM Tris, 20 mM glycine, 20% methanol). Membranes were blocked in 5% nonfat milk (20 μM Tris [pH 7.4], 0.9% NaCl, 0.1% Tween 20) and incubated with anti-pSTAT3 antibody (1:1000; Cell Signal) overnight at 4°C. Membranes were then washed and incubated with secondary antibody (anti-rabbit horseradish peroxidase coupled; 1:1000; Cell Signal), washed and developed by enhanced chemiluminescence, and imaged on the Genegnome digital imaging system (Syngene). Protein volume from the generated digital images was measured using Genetools analysis software (Syngene). For total STAT3 detection, membranes were stripped with Restore Western stripping buffer (Pierce Biotechnologies) and reprobed with an anti-STAT3 antibody (1:1000; Cell Signaling) and detected as described above.

For experiments examining the influence of subcutaeuous leptin treatment on TH and phosphoTH protein levels, mice were sacrificed following 3 days continuous minipump infusion (see above, Subcutaneous Leptin Infusion). Microdissections from the VTA, MBH, and NAc (1.5 mm diameter punch) were processed as described above. Protein samples (30 μg) were separated by SDS-PAGE, transferred to membrane and then probed for TH (1:1000; Chemicon), phosphoTH (ser40) (1:1000; Chemicon). Equal loading and transfer was verified by probing for the housekeeping protein, GADPH (1:1000; Imgenex Corp).

Combined Retrograde Tracing and Immunohistochemistry

To determine whether cells targeted by leptin project to the Nac, we combined retrograde tract tracing with pSTAT3 immunohistochemistry. Fourteen male C57BL/6J mice anesthetized with ketamine/xylazine (45 mg/kg/5 mg/kg, i.p.) received unilateral injections of rhodamine-filled latex microbeads (Retrobeads, Lumafluor Inc.) into the NAc. With the aid of an Ultraprecise Small Animal Stereotaxic Instrument (Kopf), injections were made using a 1 μl Hamilton digital syringe attached to a pulled glass micropipette with a 60–80 μm external tip diameter. The coordinates for NAc injections were 0.4 mm rostral to Bregma, 1.40 mm lateral to the midline, and 4.25 mm ventral to the skull surface, based upon the mouse brain atlas of Paxinos and Franklin (2001). The micropipette remained in place for 15 min following the delivery of 50–100 nl of tracer. The scalp incision was closed with wound clips and treated with antibiotic ointment. After a 4 to 7 day survival time, mice were fasted overnight and then injected with leptin (5 mg/kg bodyweight, i.p.). Two hours later, animals were anesthetized with ketamine/xylazine (45 mg/kg/5 mg/kg, i.p.) and underwent cardiac perfusion with ice-cold saline followed by 10% formalin. IHC procedures for pSTAT3 were as described above. Sections were mounted on gelatin-coated slides, coated with Clearmount mounting solution (Zymed), and heat-dried in an oven to form a liquid coverslip. A Zeiss A1 fluorescent microscope, Axiocam HR CCD camera, and Axiovision 4AC software (Carl Zeiss Microimaging, Inc.) was used to visualize the injection sites and the retrogradely labeled perikarya profiles in the VTA. Injection sites in which the tracer did not target any part of the NAc served as negative controls. Colocalization of tracer with pSTAT3 in the VTA was visualized and photographed with a Zeiss LSM META 510 confocal microscope and LSM META software (Carl Zeiss Microimaging, Inc.). Counts of rhodamine-labeled cells and pSTAT3 double-labeled cells in the VTA were made in sections corresponding to five different coronal levels of the A10 DA region according to the mouse atlas of Paxinos and Franklin (2001) (described here as distance caudal to Bregma): −3.08 mm, −3.16 mm, −3.40 mm, −3.64 mm, 3.80 mm. The percentage of rhodamine-labeled perikarya in the A10 region that expressed pSTAT3 was calculated.

Amphetamine-Induced Locomotor Activity and Sensitization

The experiment described here used a Comprehensive Lab Animal Monitoring System (CLAMS; Columbus Instruments) that consists of individual live-in cages for mice that allow automated, noninvasive data collection. The system allows measurement of locomotor activity by quantifying beam breaks in x-y-z planes. A total of 32 drug naïve mice (16 *ob/ob* and 16 wild-type controls) were tested. Mice were initially placed in dummy acclimation chambers for 2 days. On the third day, a 14 day Alzet micro-osmotic pump (model 1014D, Alza Corp.) was implanted SQ in the intrascapular region under Isoflurane anesthesia. The pumps delivered either leptin (500 ng/hr; 12 μg/day) or PBS for the duration of the experiment (11 days). Over the subsequent 10 days, all mice received four i.p. injections, each separated by 3 days, in the following order: (1) saline, (2) 1 mg/kg amphetamine, (3) 4 mg/kg amphetamine, (4) 1 mg/kg amphetamine. Mice were acclimatized O/N to the CLAMS chambers before the injections and returned to their home cages after the activity recording. All injections were given at the same time of day which corresponded to the middle of the light phase of the cycle. Beam breaks were measured in 10 min bins for 4 hr after the injection. Body-weight values were collected daily. One-way ANOVAs with post hoc pairwise comparisons (Fisher PLSD) were used to compare activity counts from the first hour following the injection for each of the four injections. The ability of amphetamine to sensitize the locomotor response to the second low dose (1mg/kg) of amphetamine was assessed using a one-way ANOVA that compared activity counts between the first and second low dose for each treatment group.

Slice Recordings

Mice were anesthetized with ketamine (200 mg/kg IP)/xylazine (20 mg/kg IP). Upon removal, the brain was immediately placed into ice-cold and carbogenated (95% O_2, 5% CO_2) dissection solution (Pelletier/Carlen) containing 210 mM sucrose, 3.5 mM KCl, 1 mM $CaCl_2$ dihydrate, 4 mM $MgCl_2$ hexahydrate, 1.25 mM NaH_2PO_4 hydrate, 10 mM glucose, and 26 mM $NaHCO_3$. Coronal slices containing the posterior nucleus accumbens shell region, 300 μm thick, were cut using a vibratome. Following a 1 hr recovery period in carbogenated ACSF (124 NaCl mM, 2.0 KCl mM, 1.25 KH_2PO_4 mM, 2.0 $MgSO_4$ mM, 25 $NaHCO_3$ mM, 1.0 $CaCl_2$ mM, 11 glucose mM [pH 7.3]), each slice was transferred into a recording chamber maintained at 37°C. Slices were continually perfused with ACSF at a rate of 1 ml/min. A disk carbon fiber electrode, 5 μm in diameter, was placed in the posterior nucleus accumbens shell, posterior dorsomedial striatum, or medial prefrontal cortex at a depth of ~50 μm. The reference electrode (Ag/AgCl wire) was inserted into the ACSF bath. Voltage was set to +700 mV (Axopatch 200B, Axon Instr.). The bipolar stimulating electrode (diameter 0.005 inch—MS 303/3, Plastics One, Inc.) was placed within a distance of 200 μm from the carbon fiber electrode. A constant monophasic current stimulus (delivered by Isoflex stimulus isolator, AMPI Inc., controlled by a Grass Instruments S88 Stimulator) was applied through the bipolar stimulating electrode with the following stimulation parameters: 4 ms single rectangular pulse, 300 μA current; a train of five single pulses is delivered with an interstimulus interval of 5 min to allow for full recovery. Local bath application of the dopamine reuptake blocker nomifensin (3 μM) for at least 30 min was used to assess the contribution of reuptake in the evoked dopamine signal. To examine DA release in response to a stimulation pattern that approximates real-time firing rate, an additional set of recording was collected following a train of five electrical pulses of 500 μA each with an interpulse interval of 500 ms. Amperometric electrode recordings were monitored and quantified by a locally written routine on the Superscope II platform (GW Instruments). Data acquisition occurred at 50 kHz and was digitally postfiltered at 1 kHz background-subtracted cyclic voltammograms serve to calibrate the electrodes and to identify the released substance as DA.

Data Analysis and Statistics

Data analysis included spike amplitude, spike width, and number of molecules as derived by the charge of each spike. Specifically, the total charge of the event between the baseline intercepts was determined and the number of molecules estimated by the relation N = Q/nF, where Q is the charge, n the number of electrons donated per molecule, and F is Faraday's constant (96,485 coulombs per equivalent). Estimates were based on an assumption of two electrons donated per oxidized molecule of dopamine (Ciolkowski et al., 1994). Amperometric spikes were identified as events with greater than 4.5× the Rms noise of the baseline following the stimulus artifact. This cutoff excludes all transients observed during background recordings in the bath. The event width is the duration between (a) the baseline intercept of the maximal incline from the baseline to first point that exceeded the cut-off and (b) the first data point following the maximal amplitude that registered a value of ≤ 0 pA. The maximum amplitude (i_{max}) of the event is the highest value within the event. The width at half height ($t_{1/2}$) was determined by the duration of the spike trace at one-half the maximal amplitude. The five single pulses per slice were averaged into a grand mean and the two groups (*ob/ob* versus wild-type) were compared with a one-way ANOVA.

Dopamine Radioimmunoassay

Bilateral tissue punches of the NAc (1.5 mm diameter) were collected as described above (SDS-PAGE and Immunoblotting) and homogenized in 100 μl of 0.1 N HCl. Aliquots containing the homogenates were shaken for 30 min at 4°C to allow for complete lysis and then centrifuged for 15 min at 14,000 × g. Protein concentrations were measured using BCA protein assay (Pierce Biotechnology). Samples were processed according to dopamine RIA kit instructions (RE29345, IBL Hamburg) while ensuring proper standards and controls.

Acknowledgments

We are grateful to Clifford Saper for helpful comments on this paper. We would also like to thank Maia Kokoeva and Frank Marino for their help. Thanks to the Canadian Institute of Health Research for a postdoctoral fellowship supporting S.F. and grants from NIH to J.S.F. (DKR37 28082), to J.S.F., E.M.-F. and E.N.P. (DK069983), and to E.N.P. (1RO1DK065872 and Smith Family Investigator Award-Medical Foundation). J.S.F. is on the scientific advisory board of Elixir Pharmaceuticals and receives sponsored research from Takeda Pharmaceuticals.

Received: June 13, 2006
Revised: August 17, 2006
Accepted: September 5, 2006
Published: September 20, 2006

References

Ahima, R.S., Prabakaran, D., Mantzoros, C., Qu, D., Lowell, B., Maratos-Flier, E., and Flier, J.S. (1996). Role of leptin in the neuroendocrine response to fasting. Nature *382*, 250–252.

Ahn, S., and Phillips, A.G. (2002). Modulation by central and basolateral amygdalar nuclei of dopaminergic correlates of feeding to satiety in the rat nucleus accumbens and medial prefrontal cortex. J. Neurosci. *22*, 10958–10965.

Balthasar, N., Coppari, R., McMinn, J., Liu, S.M., Lee, C.E., Tang, V., Kenny, C.D., McGovern, R.A., Chua, S.C., Jr., Elmquist, J.K., and Lowell, B.B. (2004). Leptin receptor signaling in POMC neurons is required for normal body weight homeostasis. Neuron *42*, 983–991.

Bassareo, V., and Di Chiara, G. (1999). Modulation of feeding-induced activation of mesolimbic dopamine transmission by appetitive stimuli and its relation to motivational state. Eur. J. Neurosci. *11*, 4389–4397.

Baumann, H., Morella, K.K., White, D.W., Dembski, M., Bailon, P.S., Kim, H., Lai, C.F., and Tartaglia, L.A. (1996). The full-length leptin receptor has signaling capabilities of interleukin 6-type cytokine receptors. Proc. Natl. Acad. Sci. USA *93*, 8374–8378.

Beckstead, R.M., Domesick, V.B., and Nauta, W.J. (1979). Efferent connections of the substantia nigra and ventral tegmental area in the rat. Brain Res. *175*, 191–217.

Berridge, K.C., and Robinson, T.E. (1998). What is the role of dopamine in reward: hedonic impact, reward learning, or incentive salience? Brain Res. Brain Res. Rev. *28*, 309–369.

Bina, K.G., and Cincotta, A.H. (2000). Dopaminergic agonists normalize elevated hypothalamic neuropeptide Y and corticotropin-releasing hormone, body weight gain, and hyperglycemia in ob/ob mice. Neuroendocrinology *71*, 68–78.

Campfield, L.A., Smith, F.J., Guisez, Y., Devos, R., and Burn, P. (1995). Recombinant mouse OB protein: evidence for a peripheral signal linking adiposity and central neural networks. Science *269*, 546–549.

Ciolkowski, E.L., Maness, K.M., Cahill, P.S., Wightman, R.M., Evans, D.H., Fosset, B., and Amatore, C. (1994). Disproportionation during electrooxidation of catecholamines at carbon-fiber microelectrodes. Anal. Chem. *66*, 3611–3617.

Dahlstrom, A., and Fuxe, K. (1964). Localization of monoamines in the lower brain stem. Experientia *20*, 398–399.

Di Chiara, G., Bassareo, V., Fenu, S., De Luca, M.A., Spina, L., Cadoni, C., Acquas, E., Carboni, E., Valentini, V., and Lecca, D. (2004). Dopamine and drug addiction: the nucleus accumbens shell connection. Neuropharmacology *47* (*Suppl 1*), 227–241.

Elias, C.F., Aschkenasi, C., Lee, C., Kelly, J., Ahima, R.S., Bjorbaek, C., Flier, J.S., Saper, C.B., and Elmquist, J.K. (1999). Leptin differentially regulates NPY and POMC neurons projecting to the lateral hypothalamic area. Neuron *23*, 775–786.

Elmquist, J.K., Bjorbaek, C., Ahima, R.S., Flier, J.S., and Saper, C.B. (1998). Distributions of leptin receptor mRNA isoforms in the rat brain. J. Comp. Neurol. *395*, 535–547.

Elmquist, J.K., Coppari, R., Balthasar, N., Ichinose, M., and Lowell, B.B. (2005). Identifying hypothalamic pathways controlling food intake, body weight, and glucose homeostasis. J. Comp. Neurol. *493*, 63–71.

Erickson, J.C., Hollopeter, G., and Palmiter, R.D. (1996). Attenuation of the obesity syndrome of ob/ob mice by the loss of neuropeptide Y. Science *274*, 1704–1707.

Farnebo, L.O., and Hamberger, B. (1971). Drug-induced changes in the release of 3 H-monoamines from field stimulated rat brain slices. Acta Physiol. Scand. Suppl. *371*, 35–44.

Figlewicz, D.P., Evans, S.B., Murphy, J., Hoen, M., and Baskin, D.G. (2003). Expression of receptors for insulin and leptin in the ventral tegmental area/substantia nigra (VTA/SN) of the rat. Brain Res. *964*, 107–115.

Figlewicz, D.P., Bennett, J., Evans, S.B., Kaiyala, K., Sipols, A.J., and Benoit, S.C. (2004). Intraventricular insulin and leptin reverse place preference conditioned with high-fat diet in rats. Behav. Neurosci. *118*, 479–487.

Fulton, S., Woodside, B., and Shizgal, P. (2000). Modulation of brain reward circuitry by leptin. Science *287*, 125–128.

Fulton, S., Richard, D., Woodside, B., and Shizgal, P. (2004). Food restriction and leptin impact brain reward circuitry in lean and obese Zucker rats. Behav. Brain Res. *155*, 319–329.

Hajnal, A., Smith, G.P., and Norgren, R. (2004). Oral sucrose stimulation increases accumbens dopamine in the rat. Am. J. Physiol. Regul. Integr. Comp. Physiol. *286*, R31–R37.

Halaas, J.L., Gajiwala, K.S., Maffei, M., Cohen, S.L., Chait, B.T., Rabinowitz, D., Lallone, R.L., Burley, S.K., and Friedman, J.M. (1995). Weight-reducing effects of the plasma protein encoded by the obese gene. Science *269*, 543–546.

Halaas, J.L., Boozer, C., Blair-West, J., Fidahusein, N., Denton, D.A., and Friedman, J.M. (1997). Physiological response to long-term peripheral and central leptin infusion in lean and obese mice. Proc. Natl. Acad. Sci. USA *94*, 8878–8883.

Hao, J., Cabeza de Vaca, S., and Carr, K.D. (2004). Effects of chronic ICV leptin infusion on motor-activating effects of D-amphetamine in food-restricted and ad libitum fed rats. Physiol. Behav. *83*, 377–381.

Harada, K., Wu, J., Haycock, J.W., and Goldstein, M. (1996). Regulation of L-DOPA biosynthesis by site-specific phosphorylation of tyrosine hydroxylase in AtT-20 cells expressing wild-type and serine 40-substituted enzyme. J. Neurochem. *67*, 629–635.

Harris, R.B., Zhou, J., Redmann, S.M., Jr., Smagin, G.N., Smith, S.R., Rodgers, E., and Zachwieja, J.J. (1998). A leptin dose-response study in obese (ob/ob) and lean (+/?) mice. Endocrinology *139*, 8–19.

Hay-Schmidt, A., Helboe, L., and Larsen, P.J. (2001). Leptin receptor immunoreactivity is present in ascending serotonergic and catecholaminergic neurons of the rat. Neuroendocrinology *73*, 215–226.

Hernandez, L., and Hoebel, B.G. (1988). Food reward and cocaine increase extracellular dopamine in the nucleus accumbens as measured by microdialysis. Life Sci. *42*, 1705–1712.

Heusner, C.L., Hnasko, T.S., Szczypka, M.S., Liu, Y., During, M.J., and Palmiter, R.D. (2003). Viral restoration of dopamine to the nucleus accumbens is sufficient to induce a locomotor response to amphetamine. Brain Res. *980*, 266–274.

Hoebel, B.G., Monaco, A.P., Hernandez, L., Aulisi, E.F., Stanley, B.G., and Lenard, L. (1983). Self-injection of amphetamine directly into the brain. Psychopharmacology (Berl.) *81*, 158–163.

Hyman, S.E., Malenka, R.C., and Nestler, E.J. (2006). Neural mechanisms of addiction: the role of reward-related learning and memory. Annu. Rev. Neurosci. *29*, 565–598.

Jedynak, J.P., Ali, S.F., Haycock, J.W., and Hope, B.T. (2002). Acute administration of cocaine regulates the phosphorylation of serine-19, -31 and -40 in tyrosine hydroxylase. J. Neurochem. *82*, 382–388.

Kalivas, P.W., and Stewart, J. (1991). Dopamine transmission in the initiation and expression of drug- and stress-induced sensitization of motor activity. Brain Res. Brain Res. Rev. *16*, 223–244.

Kelley, A.E. (2004). Memory and addiction: Shared neural circuitry and molecular mechanisms. Neuron *44*, 161–179.

Kelley, A.E., Baldo, B.A., Pratt, W.E., and Will, M.J. (2005). Corticostriatal-hypothalamic circuitry and food motivation: integration of energy, action and reward. Physiol. Behav. *86*, 773–795.

Luquet, S., Perez, F.A., Hnasko, T.S., and Palmiter, R.D. (2005). NPY/AgRP neurons are essential for feeding in adult mice but can be ablated in neonates. Science *310*, 683–685.

Martel, P., and Fantino, M. (1996). Mesolimbic dopaminergic system activity as a function of food reward: a microdialysis study. Pharmacol. Biochem. Behav. *53*, 221–226.

Niswender, K.D., Morton, G.J., Stearns, W.H., Rhodes, C.J., Myers, M.G., Jr., and Schwartz, M.W. (2001). Intracellular signalling. Key enzyme in leptin-induced anorexia. Nature *413*, 794–795.

Paxinos, G., and Franklin, K.B.J. (2001). The Mouse Brain in Stereotaxic Coordinates (San Diego, CA: Academic Press).

Pelleymounter, M.A., Cullen, M.J., Baker, M.B., Hecht, R., Winters, D., Boone, T., and Collins, F. (1995). Effects of the obese gene product on body weight regulation in ob/ob mice. Science *269*, 540–543.

Phillipson, O.T., and Griffiths, A.C. (1985). The topographic order of inputs to nucleus accumbens in the rat. Neuroscience *16*, 275–296.

Pothos, E.N., Creese, I., and Hoebel, B.G. (1995). Restricted eating with weight loss selectively decreases extracellular dopamine in the nucleus accumbens and alters dopamine response to amphetamine, morphine, and food intake. J. Neurosci. *15*, 6640–6650.

Pothos, E.N., Sulzer, D., and Hoebel, B.G. (1998). Plasticity of quantal size in ventral midbrain dopamine neurons: possible implications for the neurochemistry of feeding and reward. Appetite *31*, 405.

Robinson, T.E., and Berridge, K.C. (2003). Addiction. Annu. Rev. Psychol. *54*, 25–53.

Robinson, S., Sandstrom, S.M., Denenberg, V.H., and Palmiter, R.D. (2005). Distinguishing whether dopamine regulates liking, wanting, and/or learning about rewards. Behav. Neurosci. *119*, 5–15.

Salamone, J.D., Correa, M., Mingote, S.M., and Weber, S.M. (2005). Beyond the reward hypothesis: alternative functions of nucleus accumbens dopamine. Curr. Opin. Pharmacol. *5*, 34–41.

Schultz, W. (2002). Getting formal with dopamine and reward. Neuron *36*, 241–263.

Scislowski, P.W., Tozzo, E., Zhang, Y., Phaneuf, S., Prevelige, R., and Cincotta, A.H. (1999). Biochemical mechanisms responsible for the attenuation of diabetic and obese conditions in ob/ob mice treated with dopaminergic agonists. Int. J. Obes. Relat. Metab. Disord. *23*, 425–431.

Sesack, S.R., and Carr, D.B. (2002). Selective prefrontal cortex inputs to dopamine cells: implications for schizophrenia. Physiol. Behav. *77*, 513–517.

Shalev, U., Yap, J., and Shaham, Y. (2001). Leptin attenuates acute food deprivation-induced relapse to heroin seeking. J. Neurosci. *21*, RC129.

Swanson, L.W. (1982). The projections of the ventral tegmental area and adjacent regions: a combined fluorescent retrograde tracer and immunofluorescence study in the rat. Brain Res. Bull. *9*, 321–353.

Tartaglia, L.A., Dembski, M., Weng, X., Deng, N., Culpepper, J., Devos, R., Richards, G.J., Campfield, L.A., Clark, F.T., Deeds, J., et al. (1995). Identification and expression cloning of a leptin receptor, OB-R. Cell *83*, 1263–1271.

Tobler, P.N., Fiorillo, C.D., and Schultz, W. (2005). Adaptive coding of reward value by dopamine neurons. Science *307*, 1642–1645.

Vaisse, C., Halaas, J.L., Horvath, C.M., Darnell, J.E., Jr., Stoffel, M., and Friedman, J.M. (1996). Leptin activation of Stat3 in the hypothalamus of wild-type and ob/ob mice but not db/db mice. Nat. Genet. *14*, 95–97.

Vezina, P. (2004). Sensitization of midbrain dopamine neuron reactivity and the self-administration of psychomotor stimulant drugs. Neurosci. Biobehav. Rev. *27*, 827–839.

Wang, G.J., Volkow, N.D., Logan, J., Pappas, N.R., Wong, C.T., Zhu, W., Netusil, N., and Fowler, J.S. (2001). Brain dopamine and obesity. Lancet *357*, 354–357.

Wise, R.A. (2002). Brain reward circuitry: Insights from unsensed incentives. Neuron *36*, 229–240.

Zaborszky, L., and Vadasz, C. (2001). The midbrain dopaminergic system: anatomy and genetic variation in dopamine neuron number of inbred mouse strains. Behav. Genet. *31*, 47–59.

Zhao, A.Z., Huan, J.N., Gupta, S., Pal, R., and Sahu, A. (2002). A phosphatidylinositol 3-kinase phosphodiesterase 3B-cyclic AMP pathway in hypothalamic action of leptin on feeding. Nat. Neurosci. *5*, 727–728.